SAND2021-15529PE

THE UNIVERSITY OF NEW MEXICO

CQuIC Center for Quantum Information and Control

Sandia National Laboratories

A Natural Rubidium Comagnetometer for Low Frequency Communications

PRESENTED BY

John Bainbridge

Organizational Overview

I. Introduction to RF Atomic Magnetometry

II. Our Magnetometer

a) Toward Operation Outside a Shield

b) The Control Architecture

III. Results so Far

IV. Future Work

a) Miniaturization

b) Testing the Servo Limits

V. Acknowledgements

Part I:Introduction to RF Atomic Magnetometry

Why an RF Optically Pump Magnetometer (OPM)?

1. Can achieve sensitivities $\sim 1 fT/\sqrt{Hz}$, comparable to superconducting quantum interference devices (SQUIDs) without need for cryogenic cooling.
   - Savukov et al. "MRI with an atomic magnetometer suitable for practical imaging applications. Jour. Mag. Res. **199-2**. (2009)
2. Nuclear magnetic resonance (NMR) and nuclear quadrupole resonance(NQR) detection.
   - Garroway et al. "Remote Sensing by Nuclear Quadrupole Resonance". IEEE Trans. Geosci. Remote Sens. **39**,1108(2001)
   - S.-K Lee et al. "Subfemtotesla radio-frequency atomic magnetometer for detection of nuclear quadrupole resonance". Appl Phys. Lett. **89,** 214106 (2006)
   - Savukov, Seltzer, and Romalis. "Detection of NMR signals with a radio-frequency atomic magnetometer". Jour. Mag. Res. **185-2** (2007)
   - Savukov et al. "MRI with an atomic magnetometer suitable for practical imaging applications. Jour. Mag. Res. **199-2**. (2009)
3. Fundamental Physics (Axion searches).
   - Bradley et al. "Microwave Cavity Searches for Dark-Matter Axions". Rev. Mod. Phys. **75**, 777(2003)
4. Radiofrequency(RF) communication with small signal amplitude.
   - Gerginov et al. "Prospects for magnetic field communications and location using quantum sensors". Rev. Sci. Inst. **88**, 125005 (2017)

RF Magnetometry

Consider the effect an RF field transverse to $\boldsymbol{B_0} = B_0 \boldsymbol{e_z}$:

$$\boldsymbol{B_{RF}}(t) = B_{RF} \sin(\omega_{RF} t)\, \boldsymbol{e_x}$$

In RWA, causes the state to precess about $\boldsymbol{B}' = \left(\boldsymbol{B}_0 - \frac{\omega_{RF}}{\gamma}\boldsymbol{e}_z\right) + \frac{1}{2}\boldsymbol{B_{RF}}$

at $\Omega' = \sqrt{(\Delta\omega)^2 + \Omega^2}$.

Where $\Delta\omega = \omega_{RF} - \omega_0$ and

$\Omega = \frac{1}{2}\gamma B_{RF}$.

Factor of $\frac{1}{2}$ because half the RF field is corotating. Other half is counterrotating, and can be neglected in RWA.

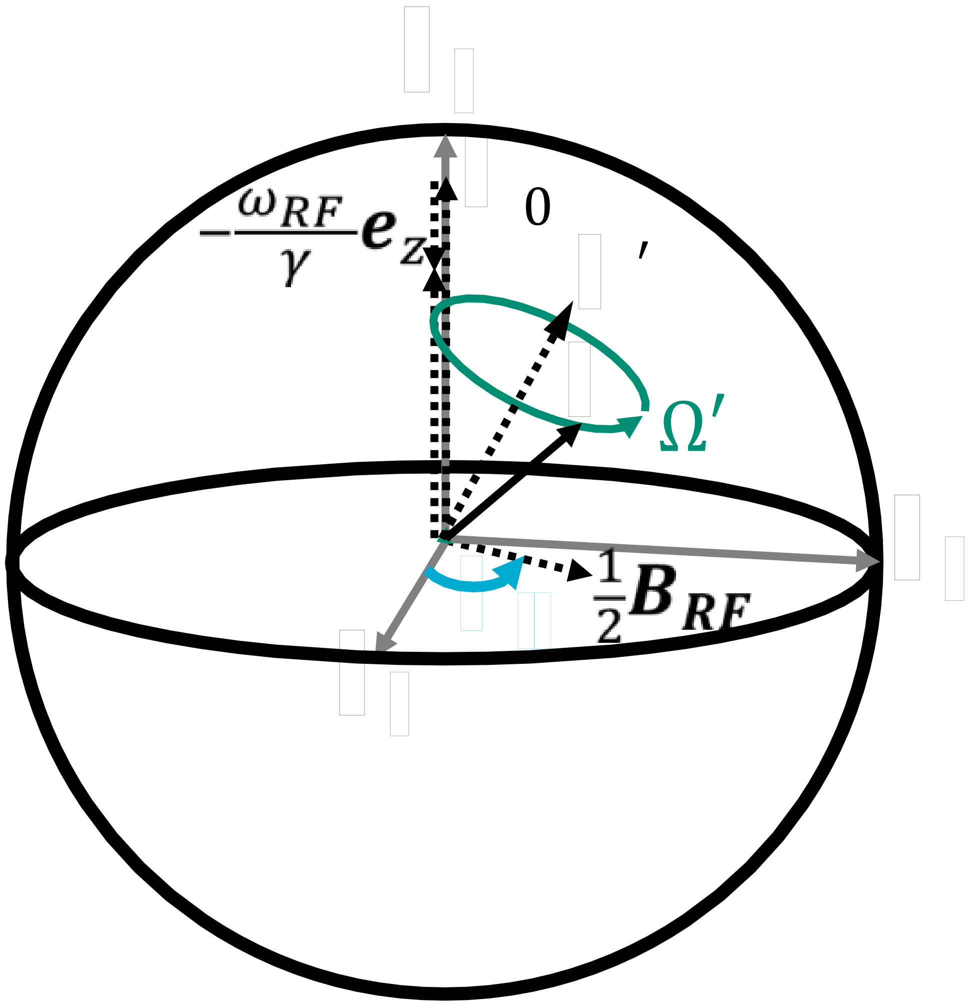

Above: Bloch sphere picture of the dynamics of the spin $\boldsymbol{S}$ in an RF magnetic field.

Practical RF Magnetometry

1. Pick frequency to measure f.
2. Tune B_0 so $2\pi f = \omega_0 = \gamma B_0$.
   - γ is the gyromagnetic ratio.
   - $\gamma = \gamma_{85} = 2\pi \times 4.67\frac{Hz}{nT}$ for ^{85}Rb.
   - $\gamma = \gamma_{87} = 2\pi \times 7.00\frac{Hz}{nT}$ for ^{87}Rb.
3. With $\omega_0 \approx \omega_{RF}$, measure

$$\langle S_x(t)\rangle = \gamma B_{Signal}[\alpha\cos(\omega_{RF}t) + \beta\sin(\omega_{RF}t)].$$

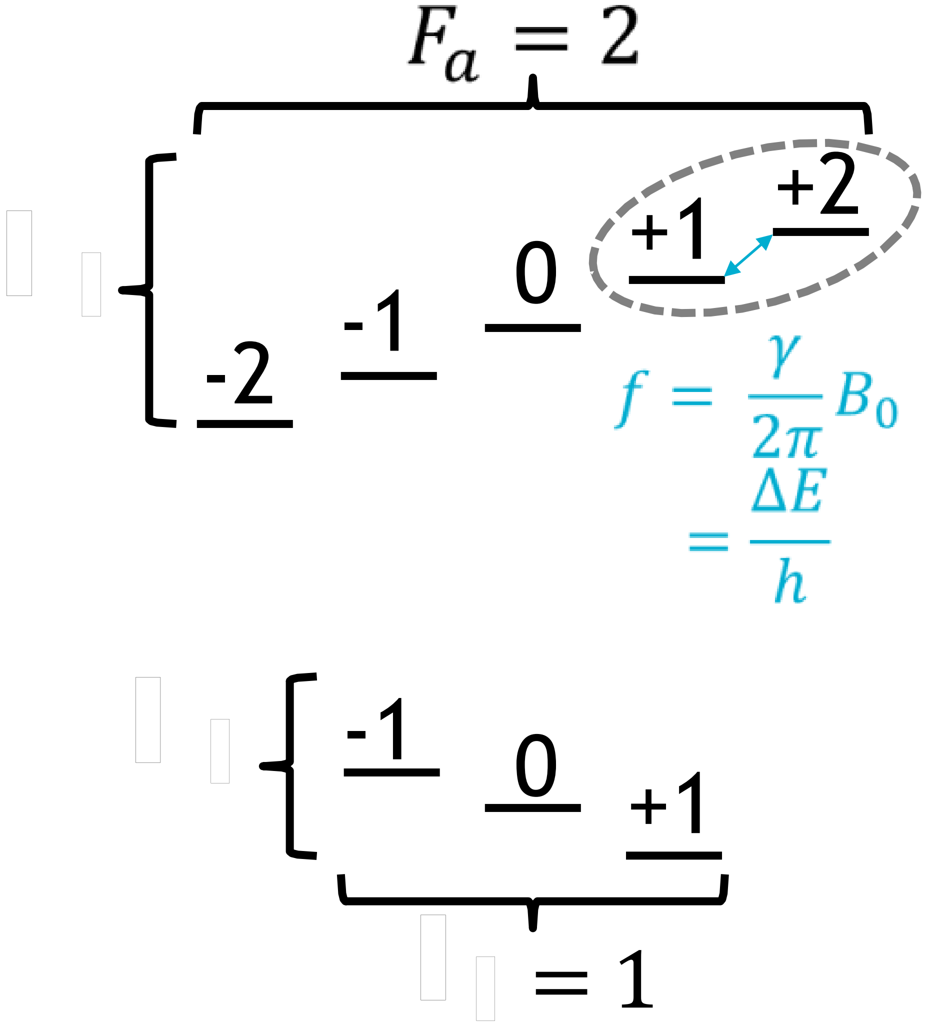

Right: Hyperfine ground state manifold of an $I = \frac{3}{2}$ alkali atom such as ^{87}Rb, with the Zeeman resonance of interest marked.

The Fundamental Sensitivity

In the limit that the hyperfine splitting >> the detection frequency >> the Zeeman linewidth, and if the atoms are pumped to be nearly completely polarized along the longitudinal direction(“z”), the sensitivity is given by the response of the transverse polarization:

$$P_x = \frac{S_x}{S_y} = \frac{1}{2}\gamma B_{RF} T_2 \sin(2\pi f_0 t)$$

- γ is the gyromagnetic ratio.
- $T_2 = \frac{1}{2\pi\Gamma_{RF}}$ is the transverse spin relaxation rate

See: Seltzer,S.J. ‘Developments in Alkali-Metal Atomic Magnetomtery.’ Ph.D thesis Princeton (2008) P 109.

Thus the sensitivity is proportional to the transverse relaxation time, so it scales inversely with the linewidth.

The Fundamental Noise Limit

The Fundamental Noise Floor

$$\delta B = \sqrt{\delta B_{SPN}^2 + \delta B_{PSN}^2 + \delta B_{LSN}^2}$$

Spin Projection Noise

Photon Shot Noise

Light Shift Noise

$$\delta B = \frac{1}{\gamma\sqrt{nV}}\sqrt{\frac{16}{(2I+1)T_2} + \frac{8}{R_{Pr}ODT_2^2\eta} + \frac{R_{Pr}OD}{2(2I+1)^2}}$$

See: Seltzer,S.J. 'Developments in Alkali-Metal Atomic Magnetomtery.' Ph.D thesis Princeton (2008) PP 114-115.

- n is the alkali density.
- V is the measurement volume.
- I is the nuclear spin.
- R_{Pr} is the off resonant depumping rate of the probe.
- OD is the optical depth.
- $\eta < 1$ is the quantum efficiency of the detector(s).

Light Narrowing

Too little optical pumping allows spin exchange collisions to distribute polarization.

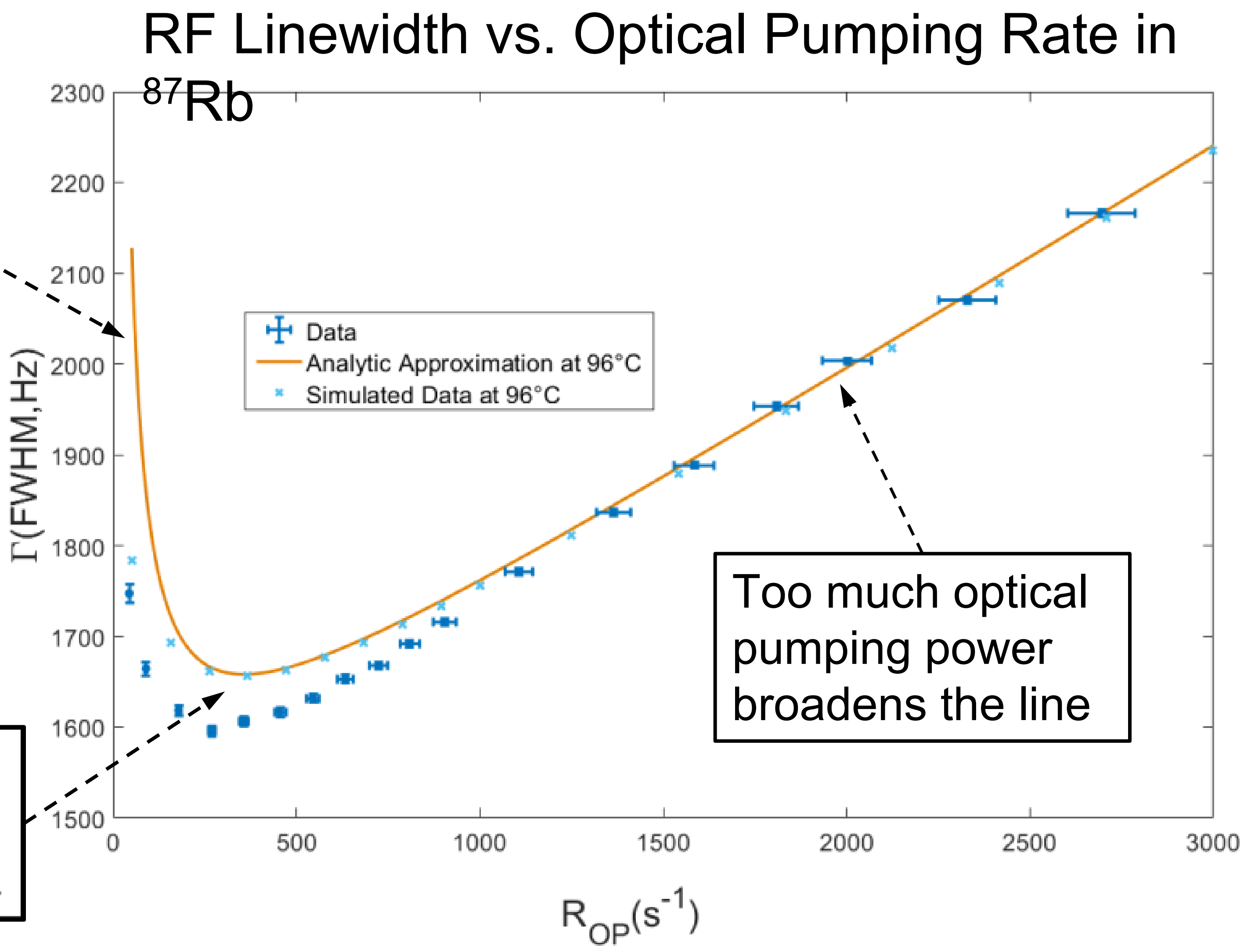

Optomized pumping rate keeps $|\psi > \approx |F = I + \frac{1}{2}, \mathrm{m_F} = \mathrm{F} >$ with minimal power broadening.

Single Species Sensitivity

Right: The response of the magnetometer to an input of $B_{Signal} \approx 47$ pT. This is comparable to the result of Savukov et al. who demonstrated a 5 $\text{fT}/\sqrt{Hz}$ sensitivity in an Rb magnetometer.[8]

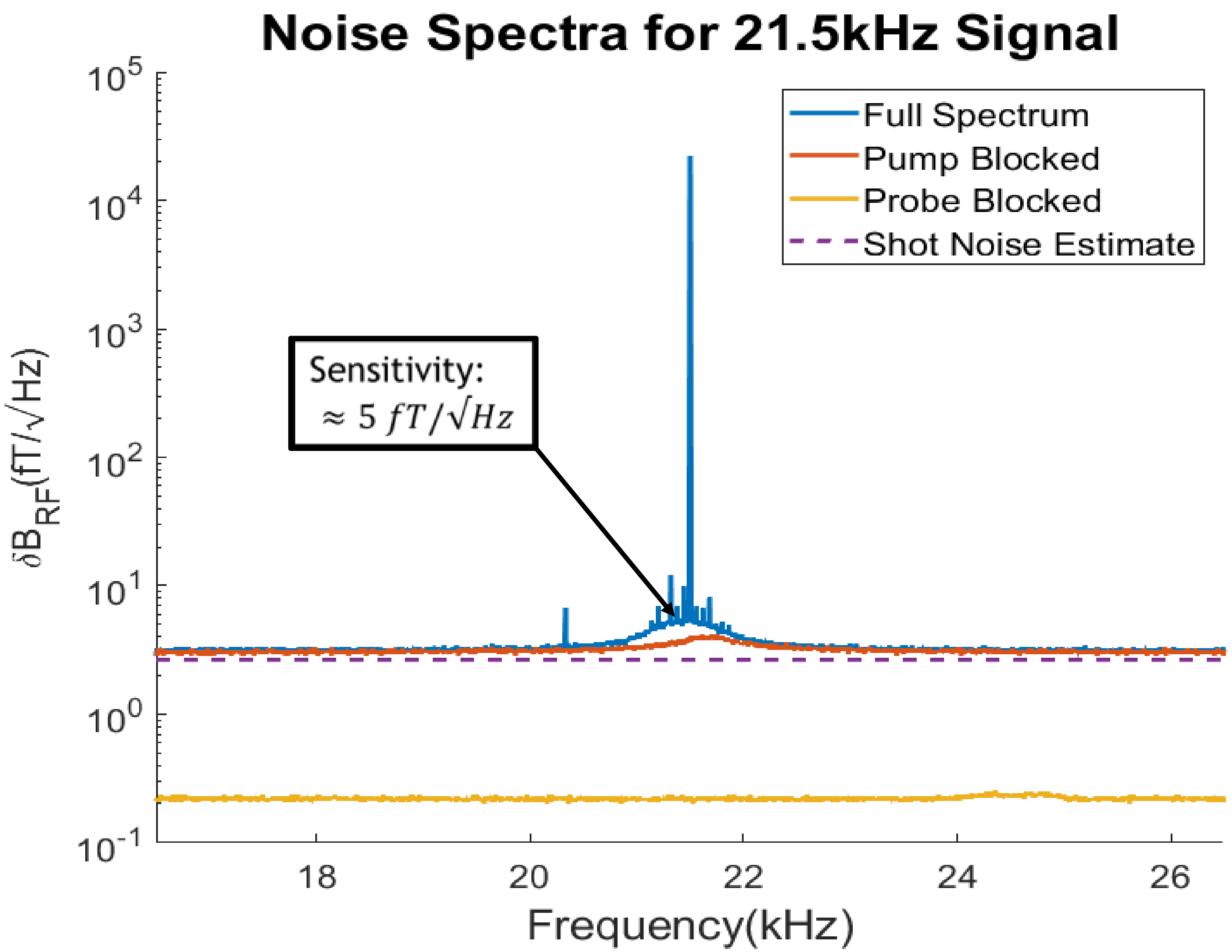

Part II(a): Operating Outside a Shield

The Problem of Unshielded Operation

- To act as a receiver, the magnetometer *must* operate outside a shielded environment!
  - An antenna inside a shield is pretty useless.
- Earth's field now adds to the bias. The total field becomes $\boldsymbol{B}_{Tot} = \boldsymbol{B}_0 + \boldsymbol{B}_{RF} + \boldsymbol{B}_{Earth} \approx \boldsymbol{B}_0 + \boldsymbol{B}_{Earth}$
  - For 21.5kHz operation, $B_0 = 4.6\ \mu T \gg B_{RF}$.
  - In Albuquerque, $B_{Earth}{\sim}60\ fT$.
  - That means $\frac{B_{Earth}}{B_0}{\sim}10$! Flirting with the regime $B_{Earth} \gg B_0$.
- To operate unshielded, active cancellation of Earth's magnetic field (along with any other external fields) <u>will be required.</u>

The OPM Variometer to Monitor External Fields

- A vector magnetometer *variometer* tracks all three external field components.
- E.B. Alexandrov et al invented an OPM implementation.
  - See E.B. Alexandrov et al, "Three-component variometer based on a scalar potassium sensor" Meas. Sci. Technol. **15** 918 (2004).
- Creates a small rotating component in the transverse plane: $\boldsymbol{B}_\perp = B_\perp(\hat{x}\sin(2\pi f_\perp t) + \hat{y}\cos(2\pi f_\perp t))$
  - $f_\perp = 500\text{ Hz} - 1\text{ kHz} \ll f_{RF}$.
- Fields transverse to $\mathbf{Z}$ will tip the plane of rotation, creating an error $\mathrm{E} \propto \mathbf{\Delta B}$.
- Demodulation with respect to $f_\perp$ will produce an error signal.
  - In-phase(I) part can be used for one direction(say '$\mathbf{X}$').
  - In-quadrature(Q) part can be used for orthogonal direction(say '$\mathbf{Y}$')

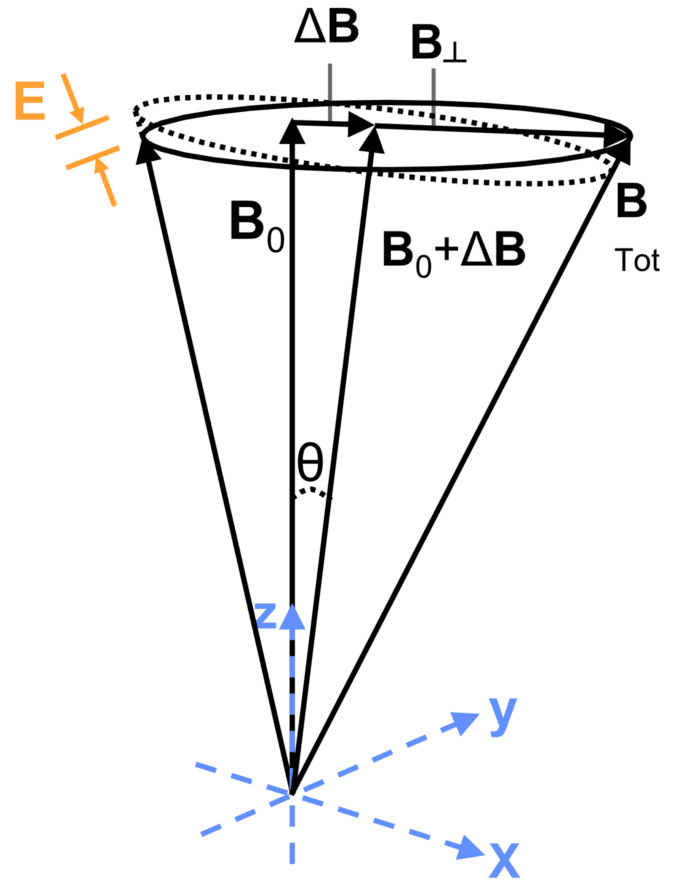

$$\mathbf{B}_{\mathrm{Tot}} = \mathbf{B}_0 + \mathbf{\Delta B} + \mathbf{B}_\perp$$

$$\rightarrow \mathbf{\Delta B} = \mathbf{B}_{\mathrm{Tot}} - (\mathbf{B}_\perp + \mathbf{B}_0)$$

The Variometer Continued: Triaxial Sensing

- Shown right is a block scheme of the variometer.
- A phase-locked loop(PLL) provides the instantaneous Larmor frequency.
  - Proportional to the *total* field.
- Using the methods described on the last slide, signals proportional to both transverse components are derived.
- Using total field and both transverse components allows for reconstruction of longitudinal field.
  - That’s all three axes.

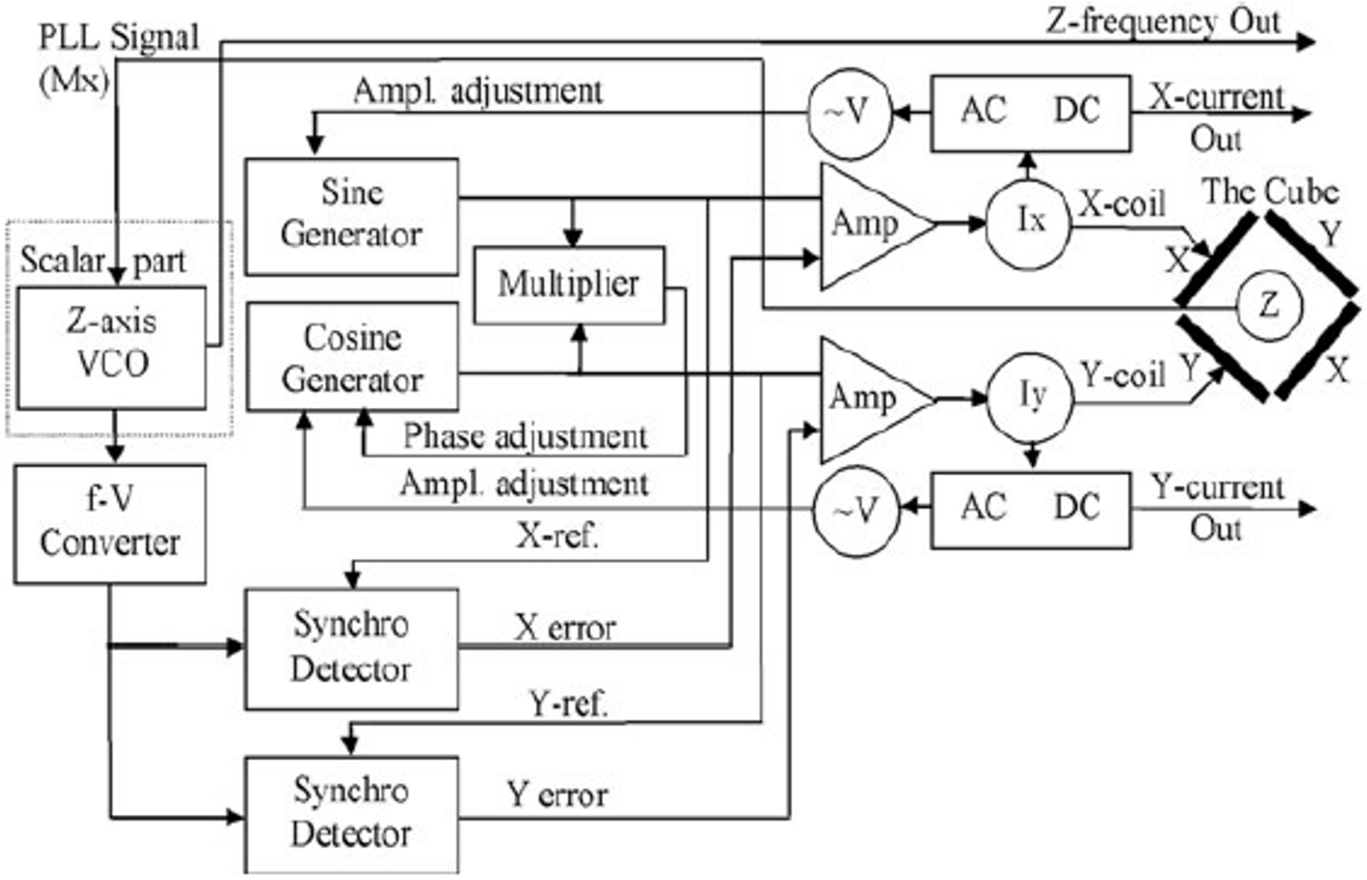

Figure 3. Block scheme of the K-variometer.

Figure from Alexandrov et al.

The Possibilities of Natural Abundance Rubidium

- Natural Rb is mostly (≈72%) ^{85}Rb, so we use it to make the high sensitivity RF magnetometer.
- There is also ≈28% ^{87}Rb.
- The ratio of gyromagnetic ratios is: $\frac{\gamma_{87}}{\gamma_{85}} = \frac{\frac{\gamma_e}{2(3/2)+1}}{\frac{\gamma_e}{2(5/2)+1}} = \frac{3}{2}$.
  - Creates a useable separation of signals in frequency space!
  - For our test signals at 21.5 kHz, ^{87}Rb is resonant at 32.25 kHz.
- We can use ^{87}Rb to create a second OPM to actively stabilize ^{85}Rb for communication.
  - Based on a modified variometer concept.

Novel Concept: Dual-isotope Comagnetometer

2-species cell enables unshielded RF magnetometer operation

$$f_{85} = \frac{2}{3} f_{87} = \frac{2}{3}\frac{\gamma_{87}}{2\pi} B$$

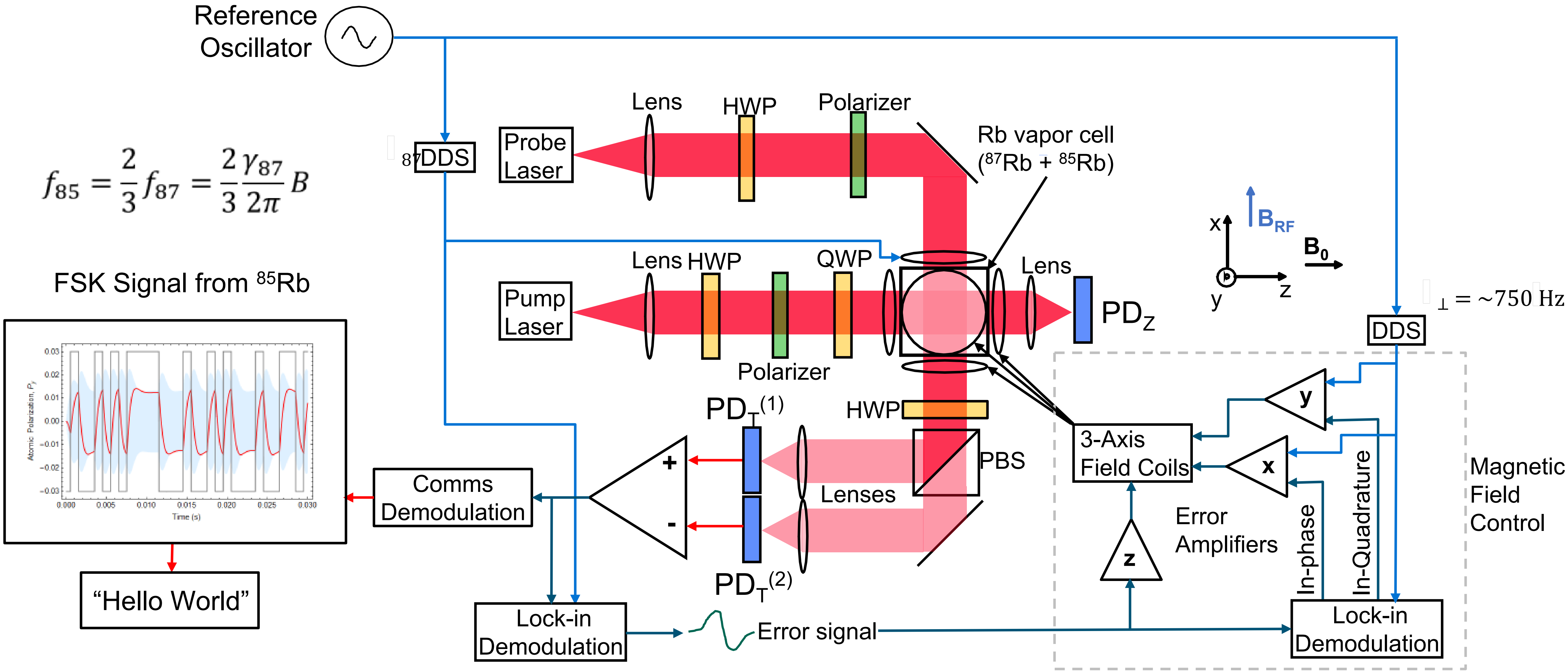

Part II(b): The Control Architecture

Fast Digital Control via an FPGA Platform

Uses the NI-7857 Reconfigurable multifunction FPGA I/O board from NI

- Integrated DAC and ADC provides eight analog in and out channels each(16 bit resolution)
- LabVIEW FPGA program generates analog outputs and processes input.
  - Same board responsible for I/O: no external phase reference required!
  - FPGA operating multiple loops to generate, sample, & process all inputs and outputs at ≥10x the highest frequency
- ‘Host’ side VI runs on laptop and communicates with FPGA
  - Provides a graphical user interface(GUI) for experimental control.
  - Handles I/O between computer(slow) and FPGA(fast)
  - Used to set all controllable parameters.

The FPGA Program Structure

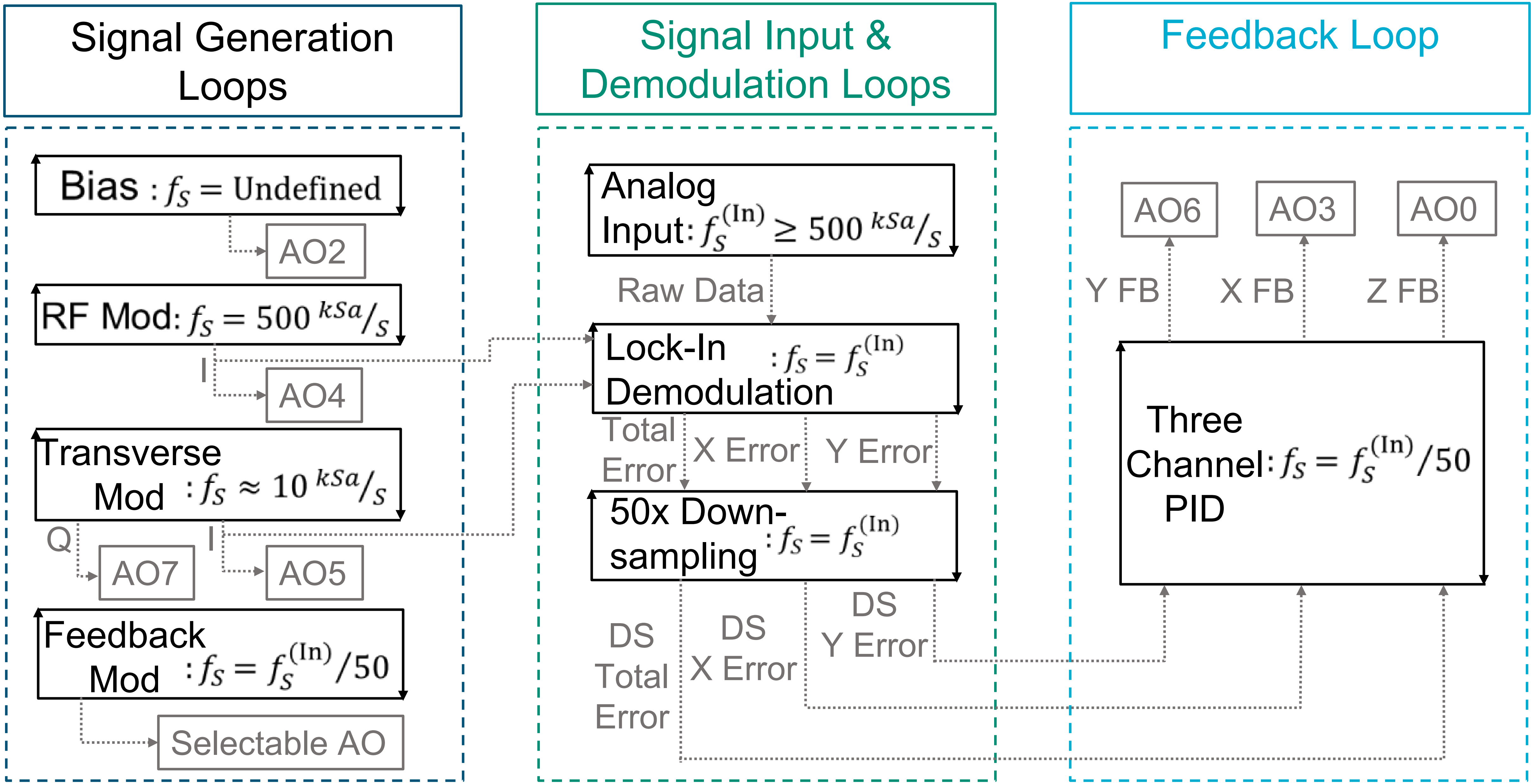

The Analog Electronics

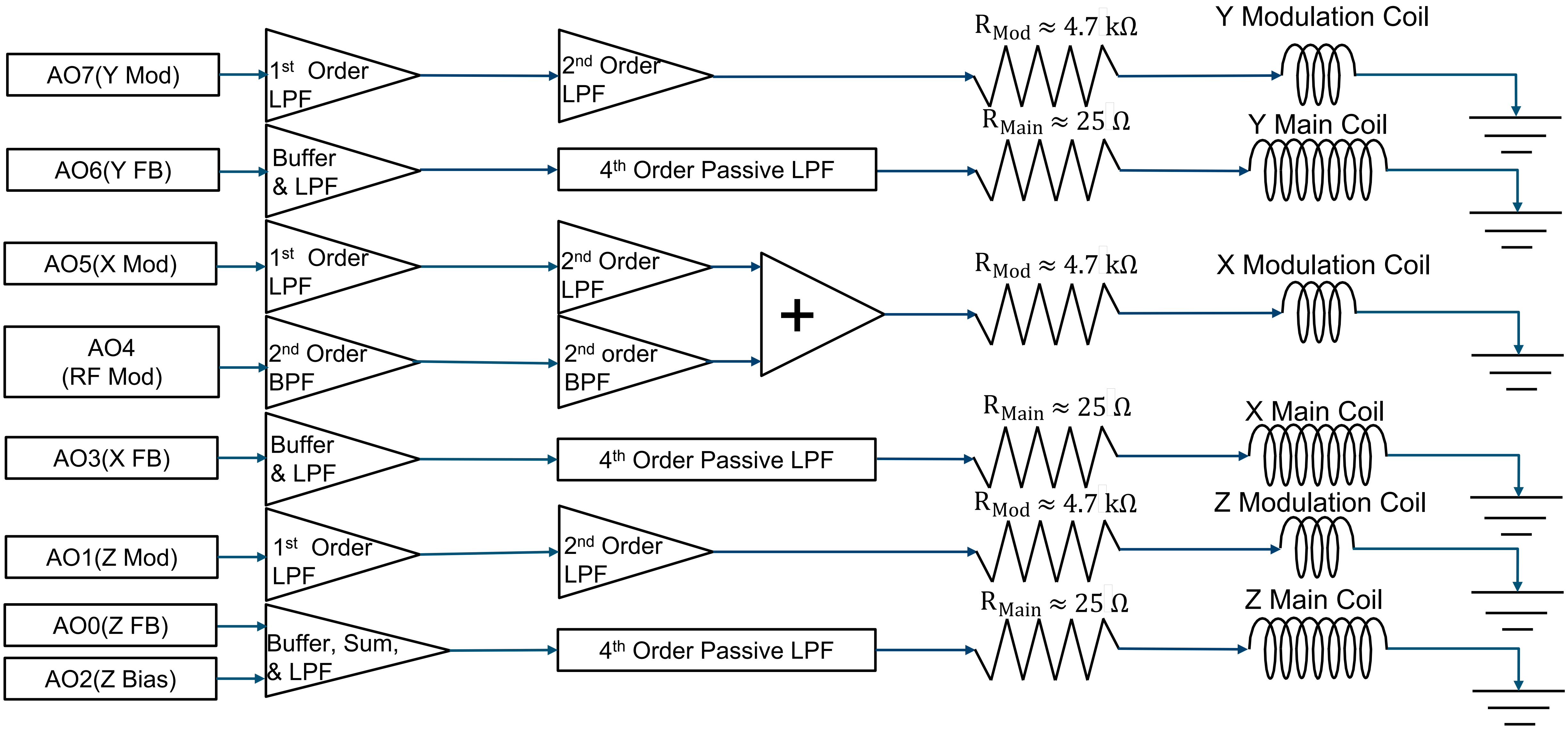

The User Interface

An example of the LabVIEW graphical user interface(GUI) for controlling the experiment via the host side VI.

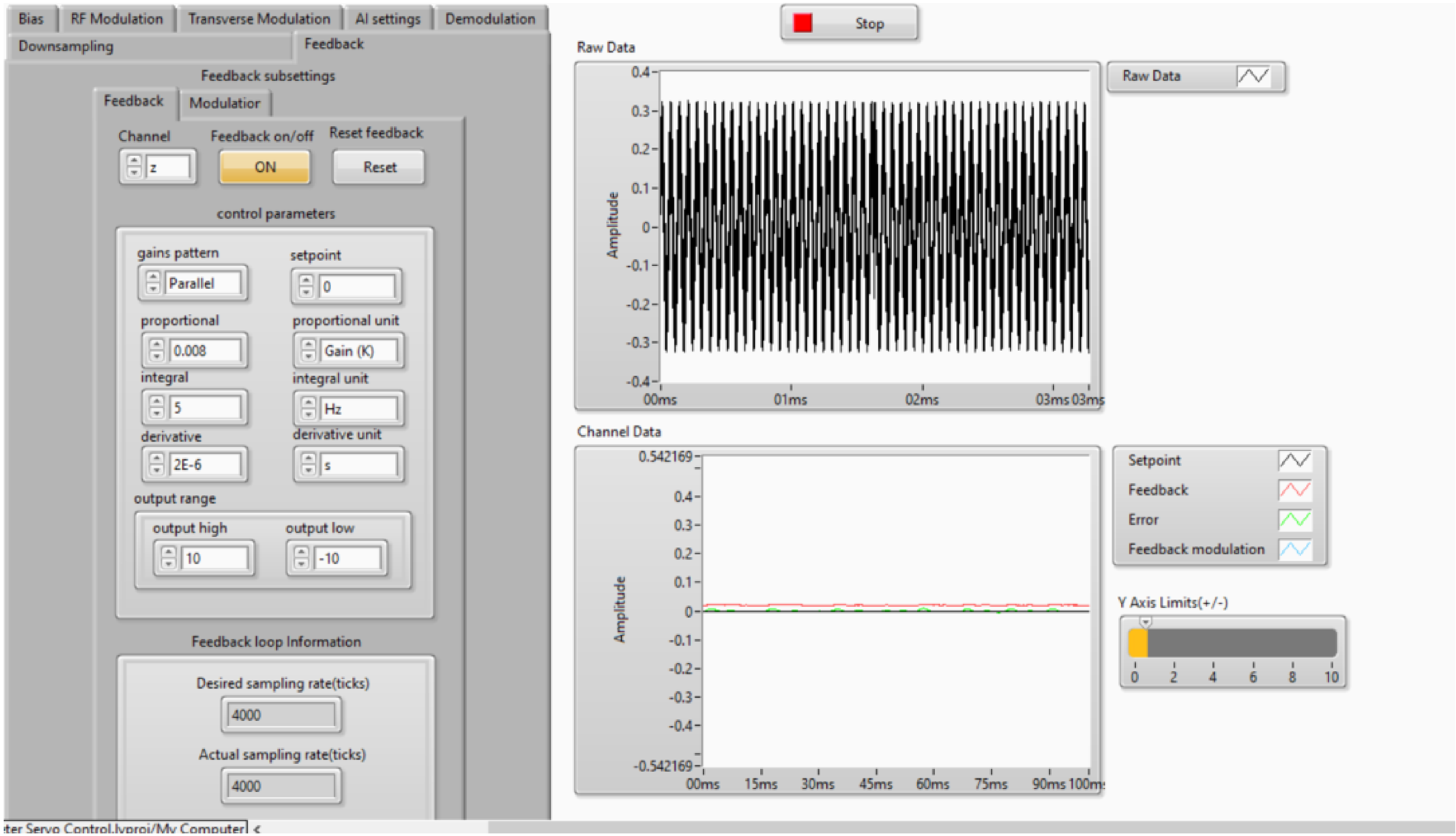

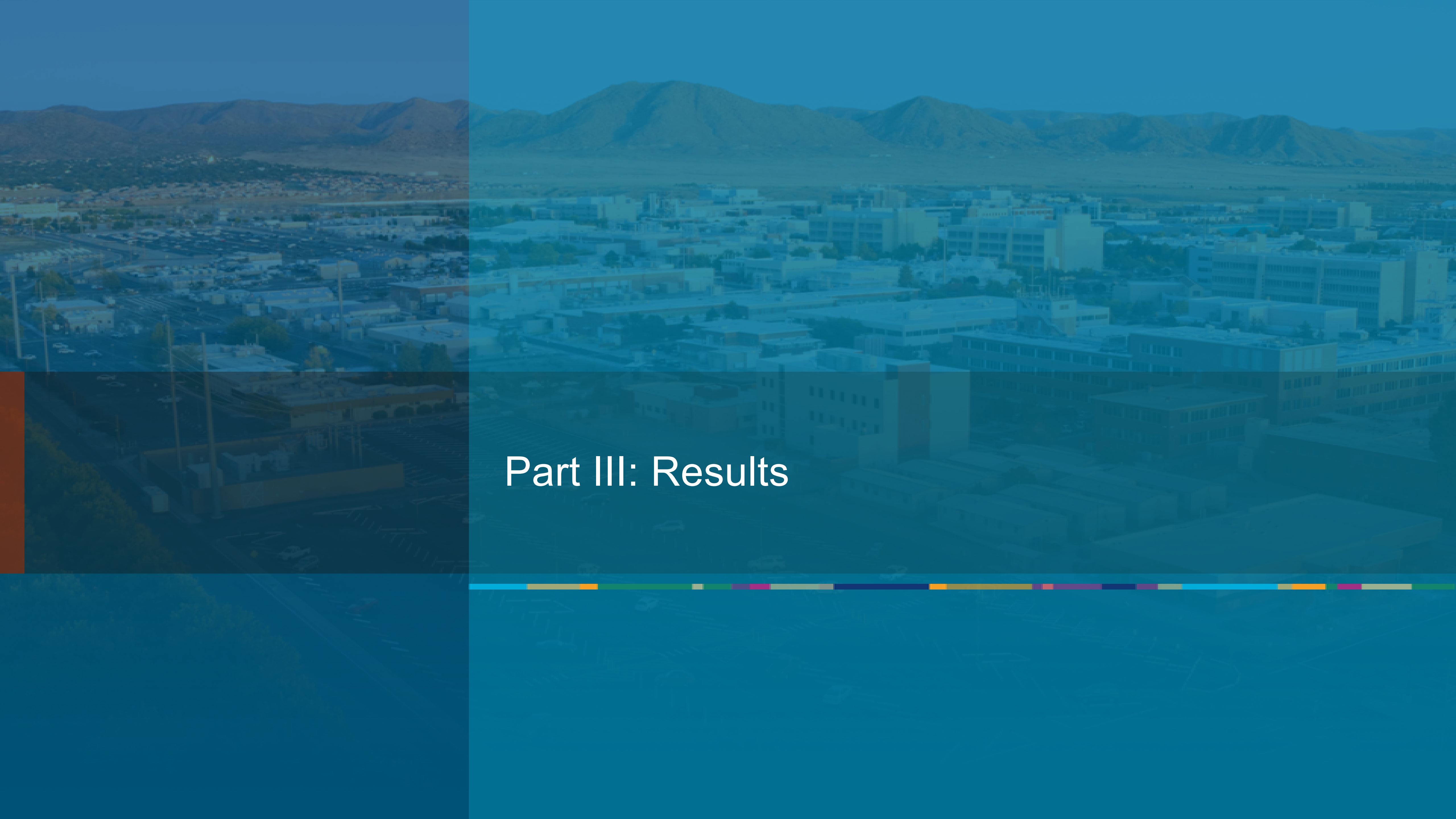

Part III: Results

Successful Servo Operation

Clockwise top-to-bottom: Successful simultaneous engagement of the longitudinal(z) and transverse x & y servos on all three channels. Results in 4-layer μ-metal shield

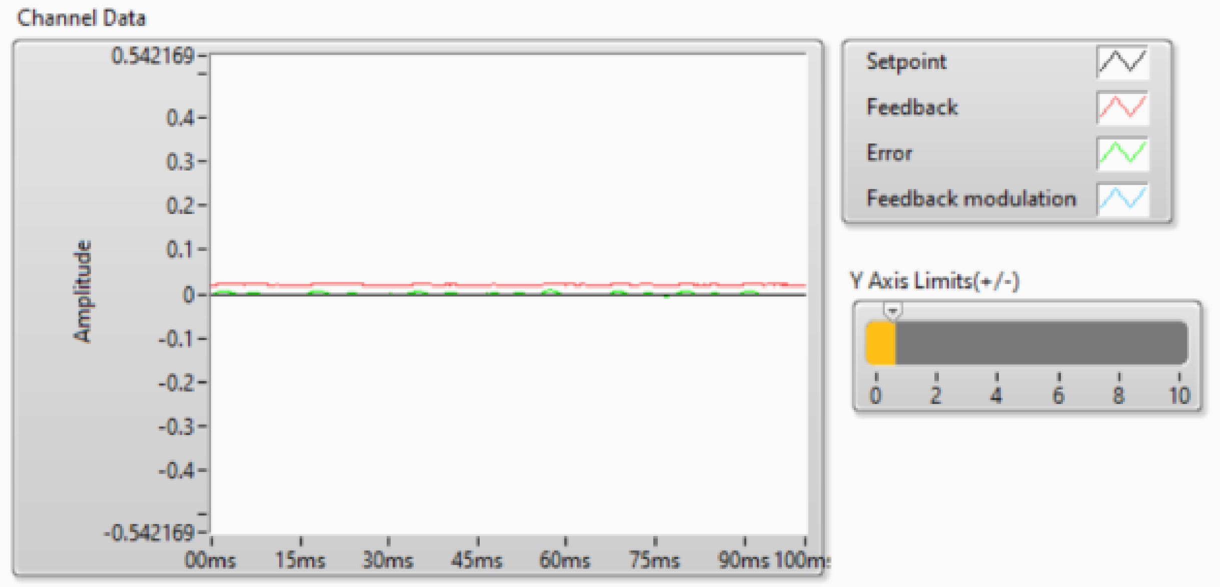

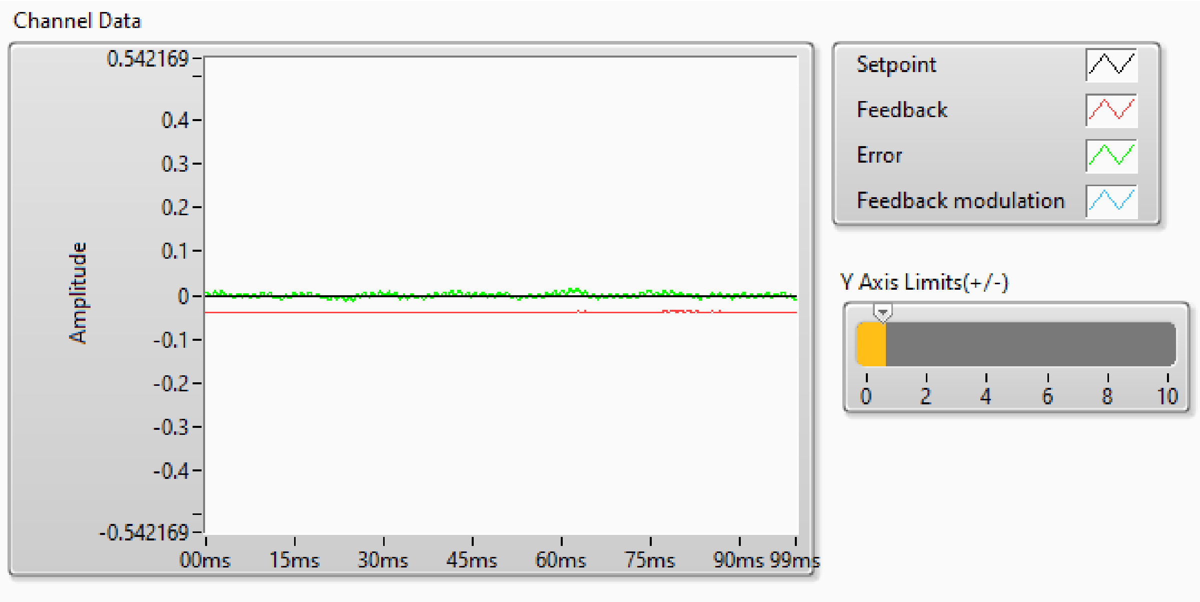

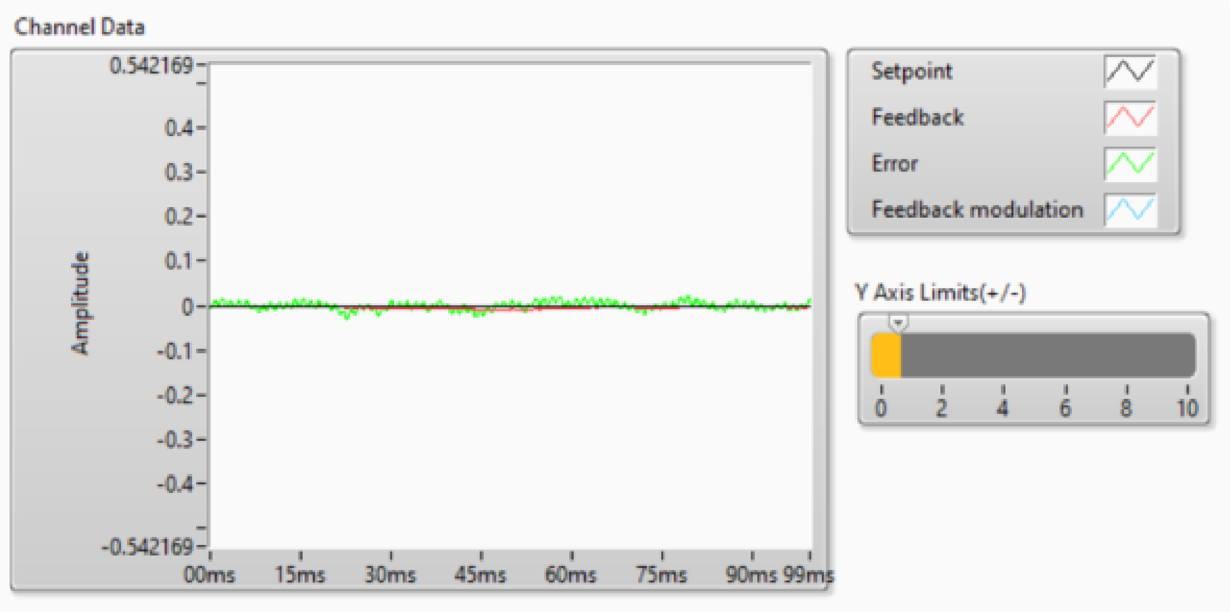

Successful Servo Operation: The Screwdriver Test

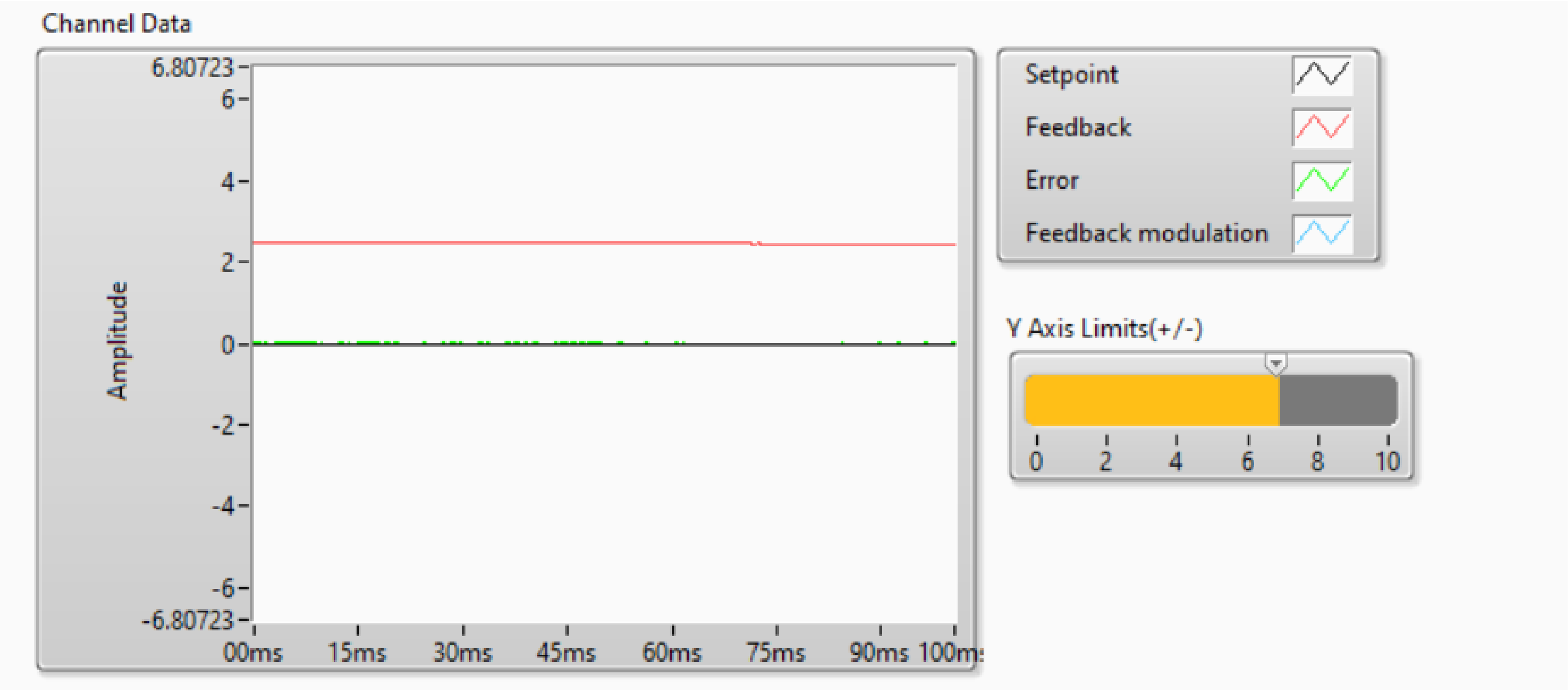

Above: The response of the vertical (y) axis servo to a magnetized object (a screwdriver) inserted vertically inside the magnetic shield. With the servo engaged, sensitivity is maintained despite the presence of the screwdriver.

Communications Testing: Minimum Shift Keying(MSK) Decoding

Right: The decoded response of the magnetometer to a simple message at various amplitudes.

Plot from Jeff Bach

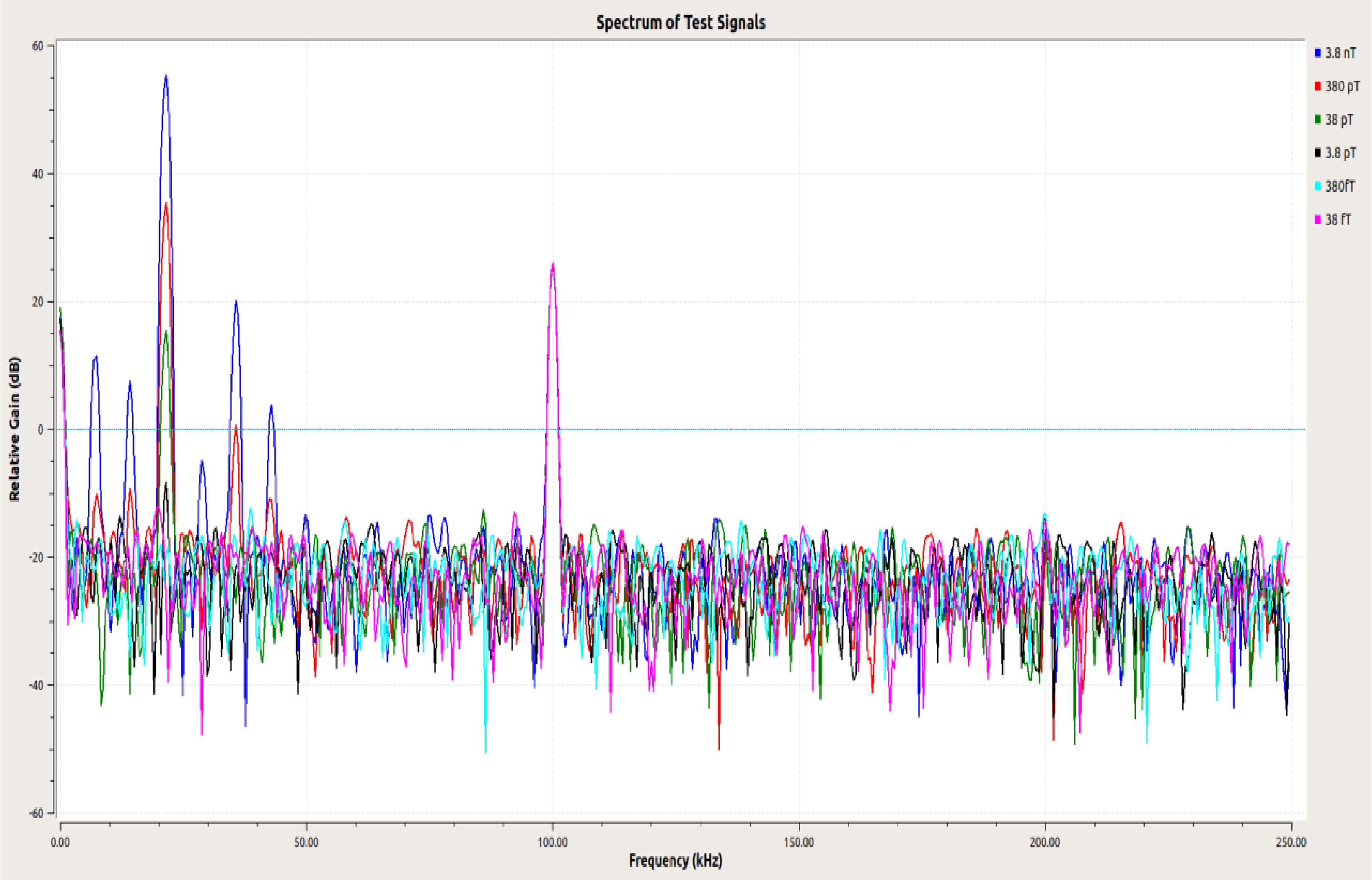

Signal Decoding: Succusses and Failures

Field Strength	Possible Bursts	Decoded Bursts
3.8 nT	10	9
380 pT	10	9
38 pT	10	9
3.8 pT	10	0
380 fT	10	0
38 fT	10	0

Left: A table showing the number of successfully decoded messages out of 10 transmitted for various signal amplitudes.

Note: The operating sensitivity of the magnetometer has been improved considerably since these data were taken. (see next slides)

Table complied by Jeff Bach.

Magnetometer Sensitivity: Servos Operational

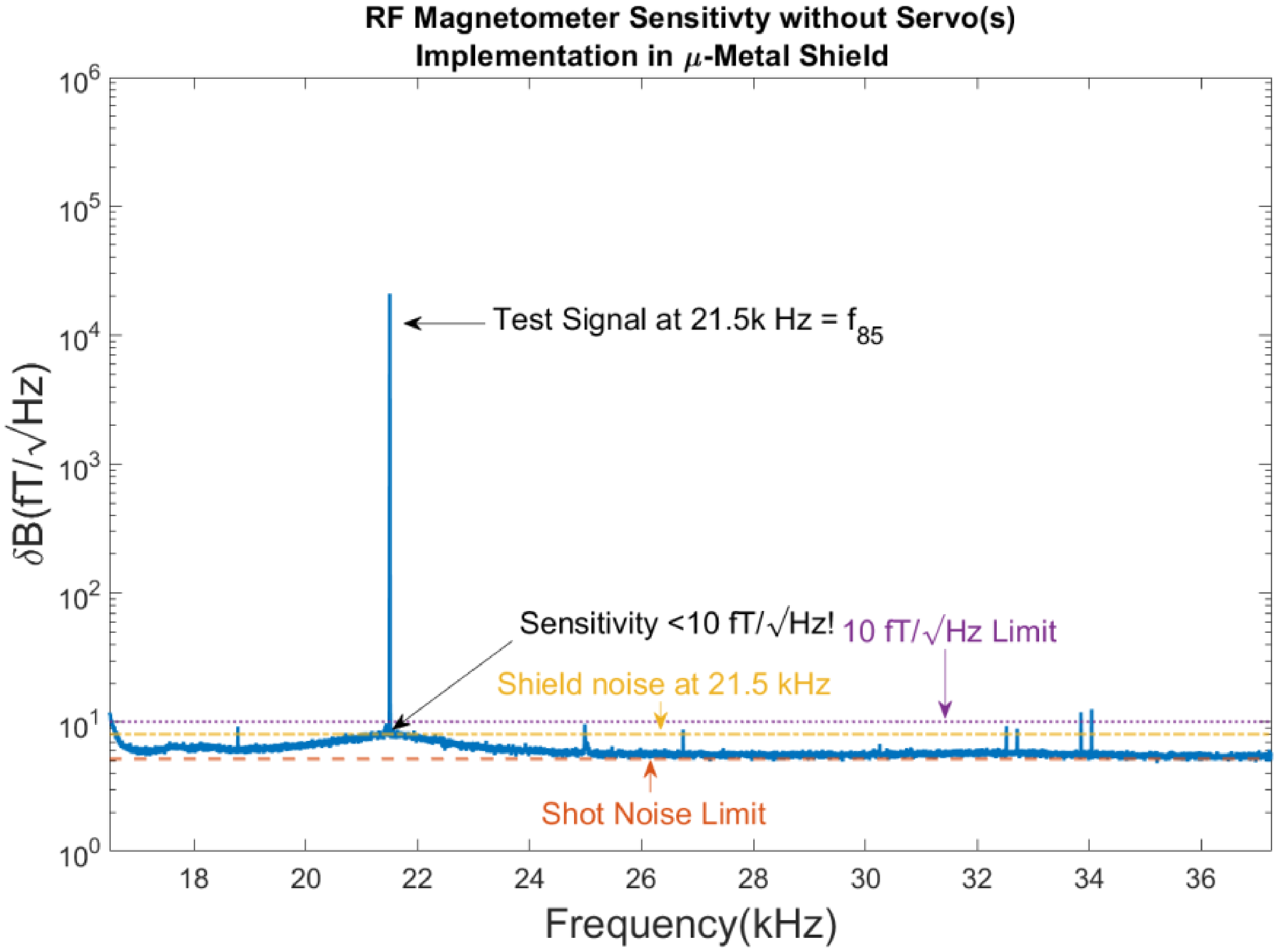

Left: Data showing the operation of the magnetometer in a shield without the servo(s) and associated modulations engaged. These data provide a baseline for comparison

Magnetometer Sensitivity: Servos Operational

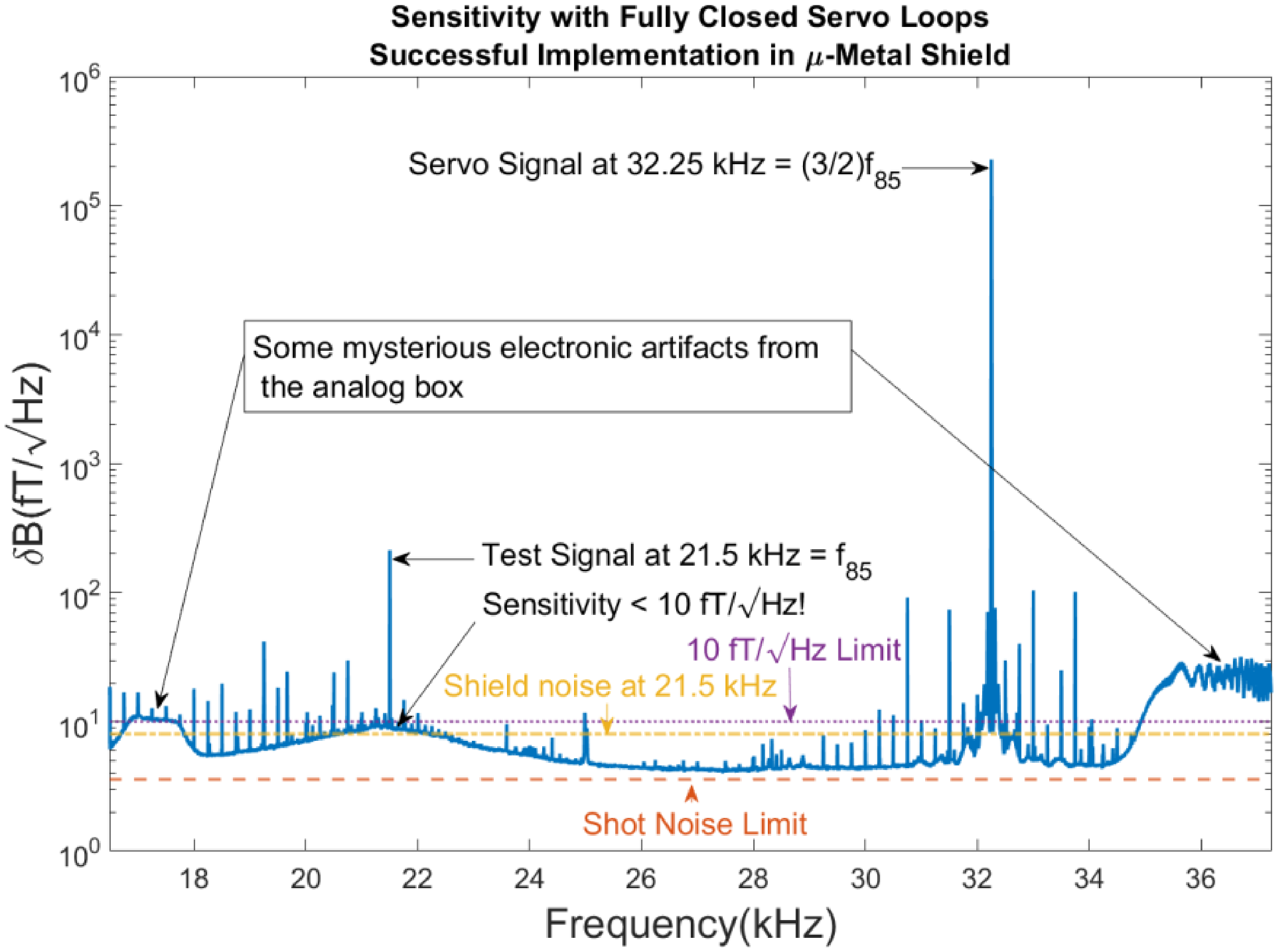

Left: Data showing the operation of the magnetometer in a shield with all servo(s) engaged while maintaining a high sensitivity. The "spikes" in the spectrum are observed to be at frequencies of the form

$$f_{Spike} = f_{Center} \pm n \cdot 60\text{Hz} \pm m \cdot f_{\perp},$$

Part IV(a): Miniaturization

Miniaturizing the Sensor

- Novel optical layout for mini RF magnetometer (volume < 600 cm^3)
- Uses 3D printed mounts; keeps lasers and PDs as far away from Rb cell as possible.

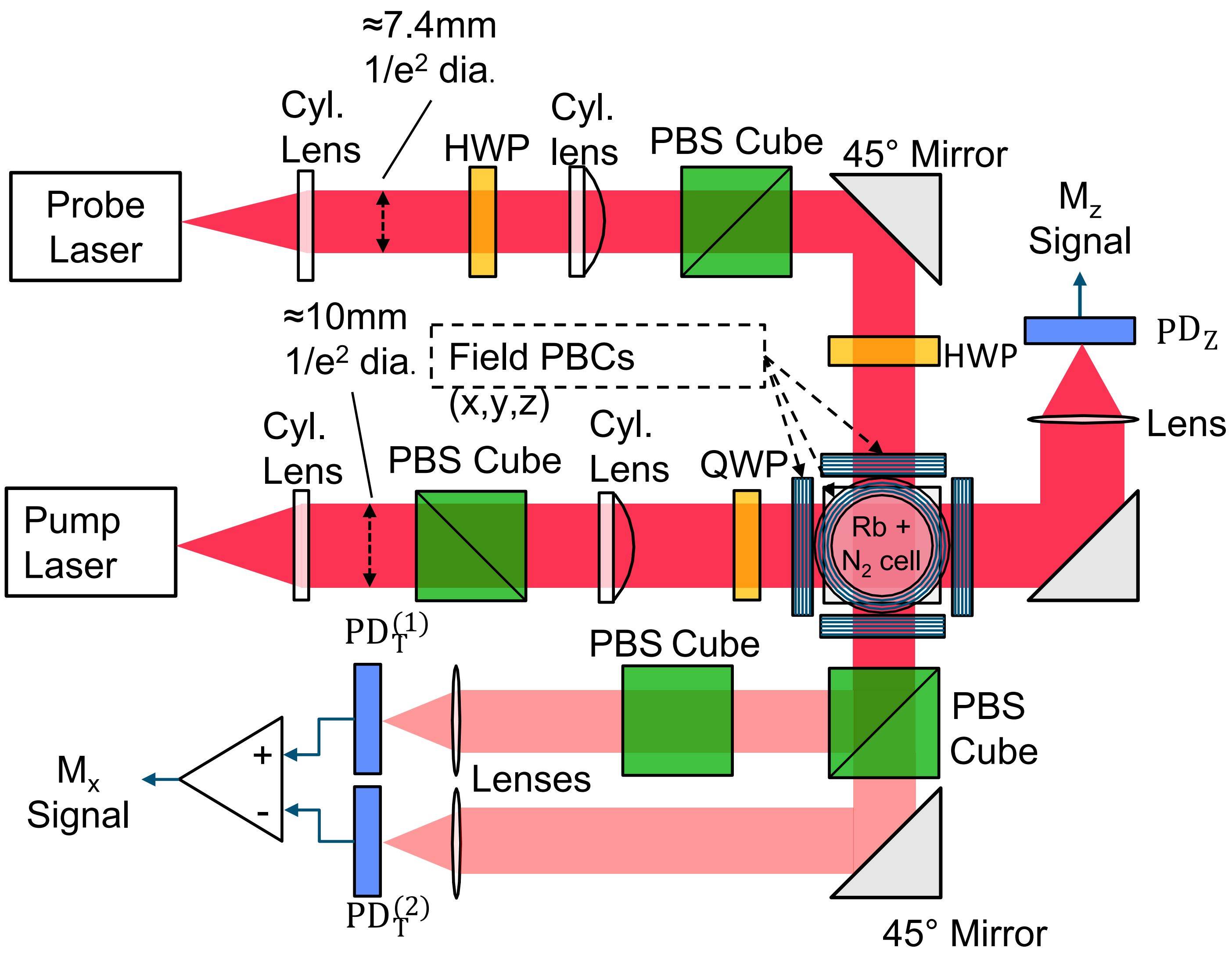

PCB's for Compact, Uniform, High-Gain Field Coil(s)

- Used bfieldtools package to design compact PCB's to produce control field(s)
  - Thanks to Joonas Iivanainen
- All faces contribute to every direction.
  - Each face has 6 layers.
- Produce highly uniform($\sim 0.5\%$) fields

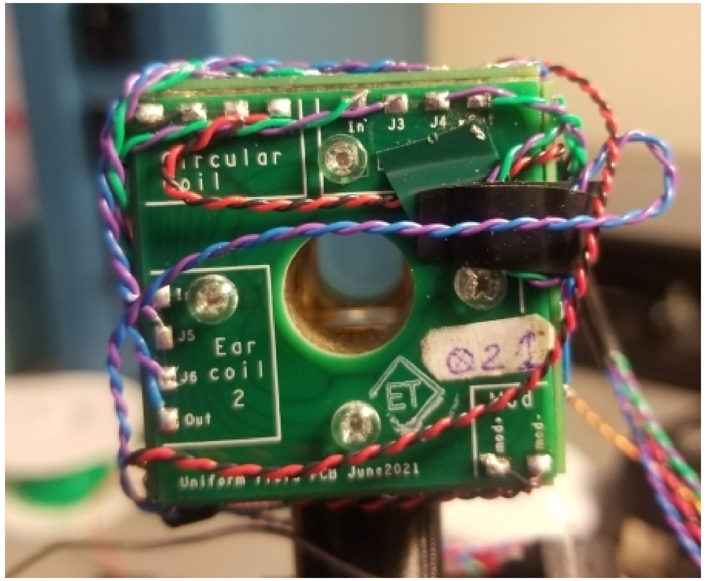

Above: The PCB's assembled around the natural Rb+N_2 cell and heater.

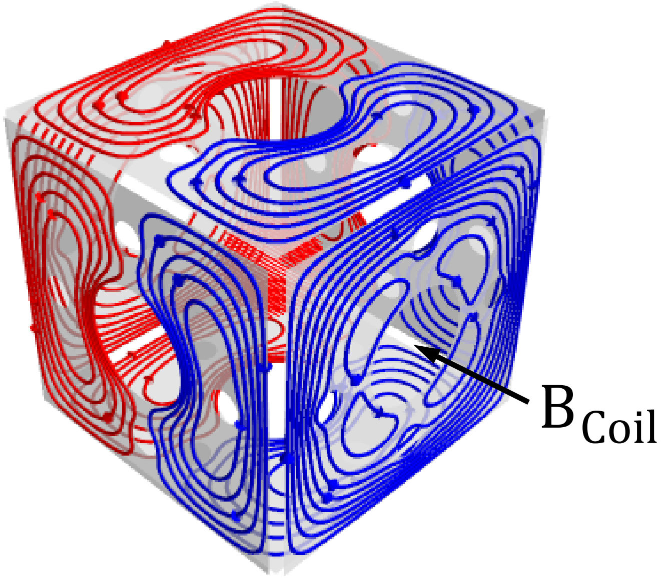

Left: Current distribution over 6 faces for a single field direction. Blue is clockwise about the outward surface normal, red is counter-clockwise.

Miniaturized Sensor Design

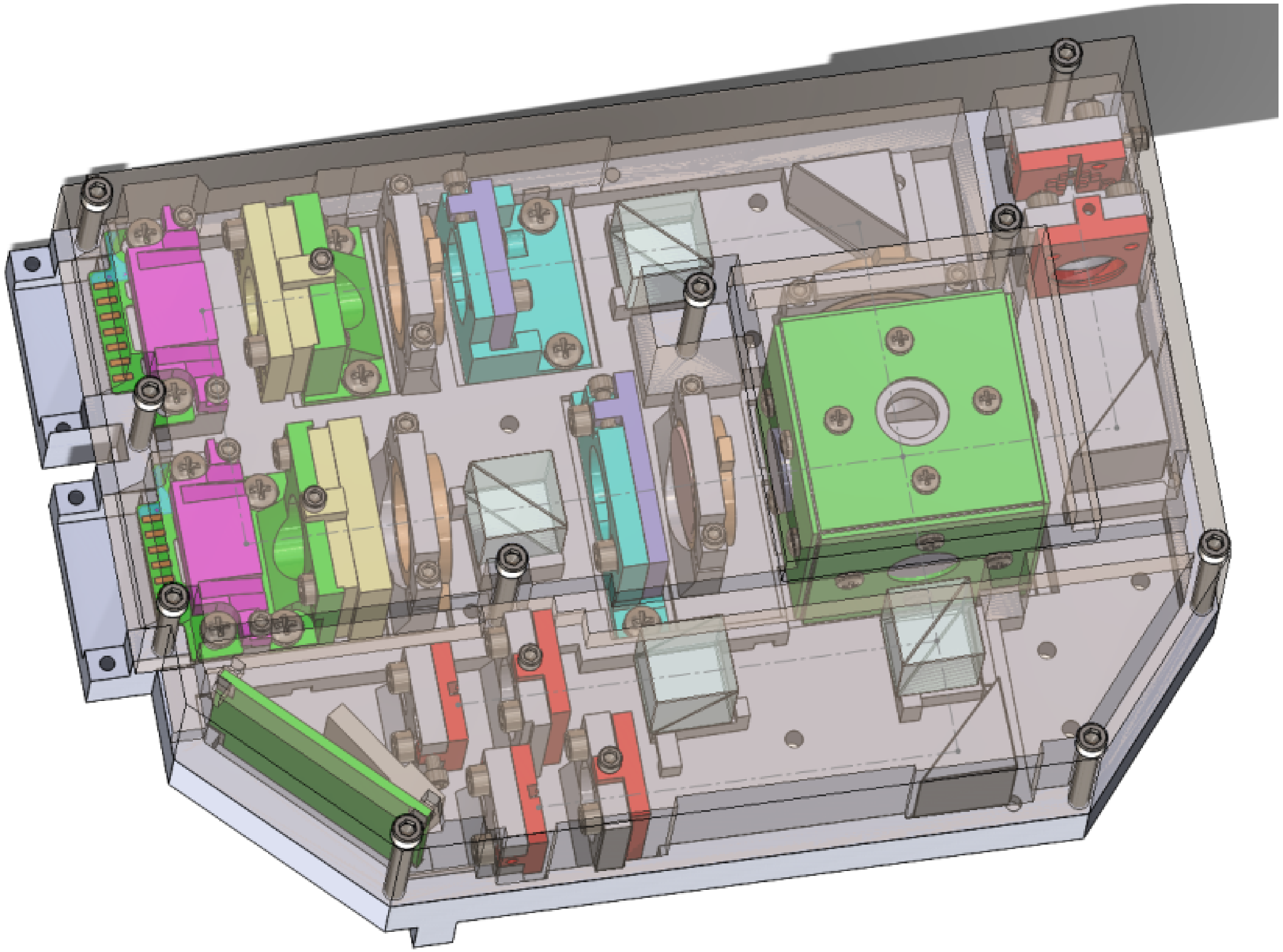

Above: *SolidWorks* rendering of miniaturized RF magnetometer sensor.

Physics Package in Progress

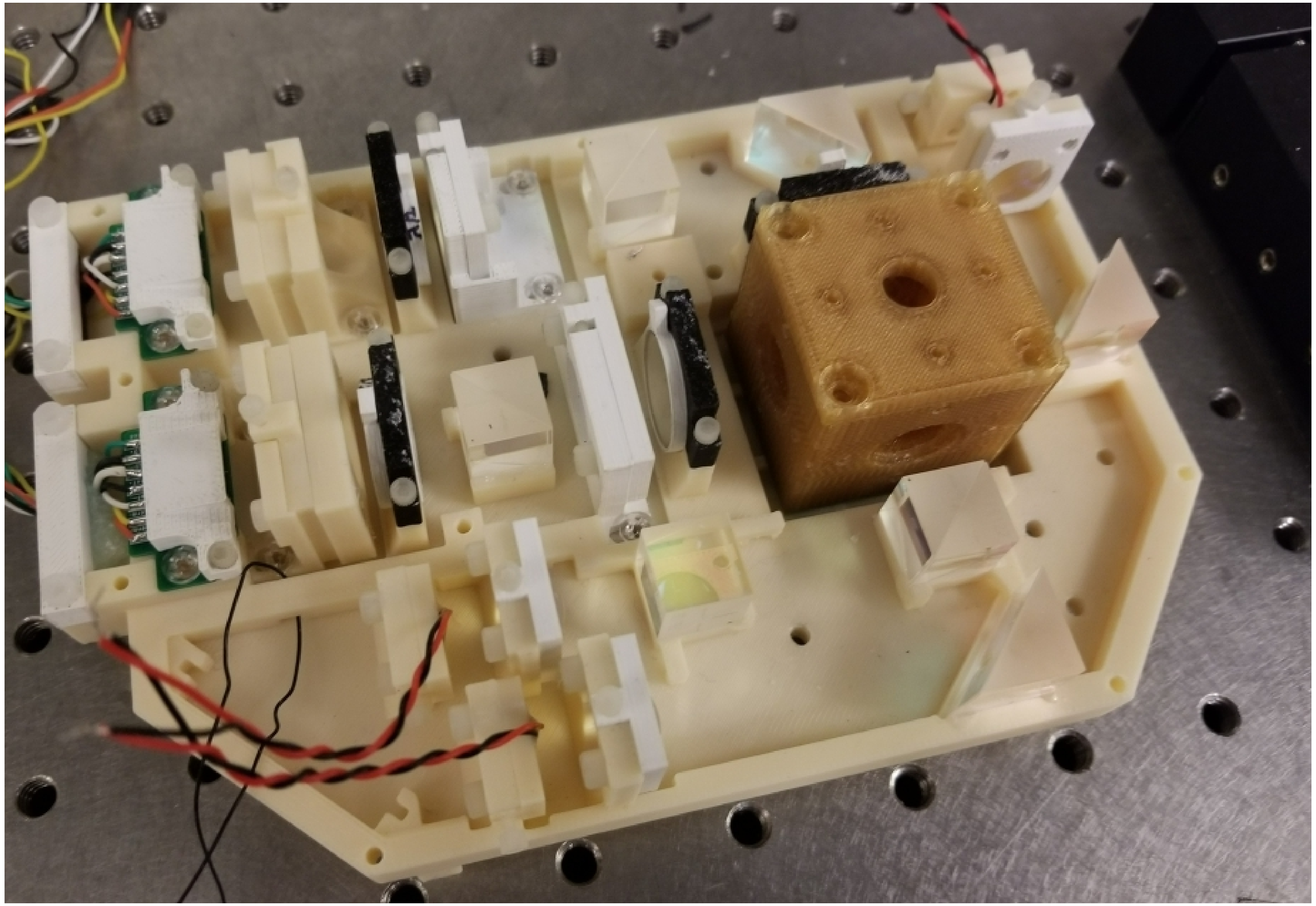

Above: The physics package in it’s current (as of 11/30/2021) sate of assembly.

Miniaturization: To Do

Complete compact mobile platform.

- Optical layout is nearly complete.
- The cell, oven, and PCB coil's must be moved into place.
- Balanced photodiode circuit on the way from Lee Marshall.
- Test compact package in shield to ensure successful operation after full assembly

Part IV(b): Test the Servo Limits

Testing the Servo(s): To Do

1. Demonstrate ability of servo to compensate slow (~5Hz) oscillating/rotating fields in shield.
   - Test field amplitudes must be on the order of Earth's field: $|B_{\text{Test}}| \sim |B_{\text{Earth}}|$
   - Show ability to servo compensate each direction individually
   - Show ability to compensate rotating field in 3 orthogonal planes (ZX,ZY,&XY)
   - Write a paper on the results.
2. Move outside for real world testing. Test decoding in various indoor/outdoor environments.
   - Write a follow-up paper and a thesis.

Part III: Acknowledgements

Acknowledgements

- Thanks to Sandia National Labs for providing funding for this work*
- Thanks to Peter Schwindt for giving me the opportunity to work on this project, and his continuing mentorship.
- Thanks to Neil Claussen for his work on various technical aspects of the project.
- Thanks to Joonas Iivanainen for his compact coil design via bfieldtools.
- Thanks to Jeff Bach for his work the communications aspects of the project.

Above: Peter Schwindt
(image by Arne Wickenbrock)

Below: Neil Claussen

*Sandia National Laboratories is a multimission laboratory managed and operated by National Technology & Engineering Solutions of Sandia, LLC, a wholly owned subsidiary of Honeywell International Inc., for the U.S. Department of Energy's National Nuclear Security Administration under contract DE-NA0003525.